AD-A039 543 RADIATION RESEARCH ASSOCIATES INC FORT WORTH TEX F/G 4/1
CALCULATIONS OF THERMAL RADIATION TRANSMISSION THROUGH CLOUDS.(U)
MAY 77 D G COLLINS F08606-77-C-0008
UNCLASSIFIED RRA-M7704 AFTAC-TR-77-16 NL

| OF |
AD
A039543

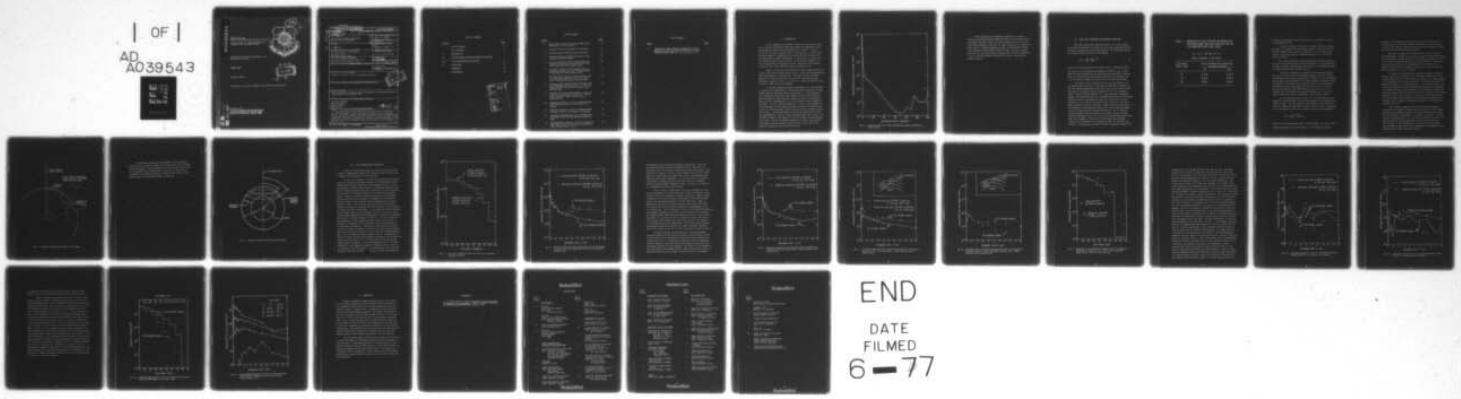

END

DATE
FILMED
6-77

AFTAC-TR-77-16

Calculations of Thermal Radiation Transmission Through Clouds

Radiation Research Associates, Inc.
Fort Worth, Texas

6 MAY 1977

Topical Report

Approved for public release; distribution unlimited.

Prepared for
AIR FORCE TECHNICAL APPLICATIONS CENTER
HEADQUARTERS UNITED STATES AIR FORCE
PATRICK AIR FORCE BASE, FLORIDA 32925

UNCLASSIFIED

SECURITY CLASSIFICATION OF THIS PAGE (When Data Entered)

REPORT DOCUMENTATION PAGE	READ INSTRUCTIONS BEFORE COMPLETING FORM
1. REPORT NUMBER: AFTAC TR-77-16	2. GOVT ACCESSION NO. / 3. RECIPIENT'S CATALOG NUMBER
4. TITLE (and Subtitle): CALCULATIONS OF THERMAL RADIATION TRANSMISSION THROUGH CLOUDS.	5. TYPE OF REPORT & PERIOD COVERED: TOPICAL rept.
	6. PERFORMING ORG. REPORT NUMBER: RRA-M7704
7. AUTHOR(s): D. G. Collins	8. CONTRACT OR GRANT NUMBER(s): F08606-77-C-0008 new
9. PERFORMING ORGANIZATION NAME AND ADDRESS: Radiation Research Associates, Inc. 3550 Hulen Street Fort Worth, Texas 76107	10. PROGRAM ELEMENT, PROJECT, TASK AREA & WORK UNIT NUMBERS: P.A. No. T/7505/T/ETR
11. CONTROLLING OFFICE NAME AND ADDRESS: Air Force Technical Applications Center Patrick Air Force Base, FL 32925	12. REPORT DATE: 6 May 1977
	13. NUMBER OF PAGES: 31 (12) 34p.
14. MONITORING AGENCY NAME & ADDRESS (if different from Controlling Office)	15. SECURITY CLASS. (of this report): Unclassified
	15a. DECLASSIFICATION/DOWNGRADING SCHEDULE

16. DISTRIBUTION STATEMENT (of this Report)

Approved for public release; distribution unlimited.

17. DISTRIBUTION STATEMENT (of the abstract entered in Block 20, if different from Report)

18. SUPPLEMENTARY NOTES

Paper presented at the Annual Satellite Diagnostic Working Group Meeting, Patrick AFB FL, 8-10 February 1977.

19. KEY WORDS (Continue on reverse side if necessary and identify by block number)

Monte Carlo Methods
Cloud Transmission
Thermal Radiation
Point Sources

294300

20. ABSTRACT (Continue on reverse side if necessary and identify by block number)

This paper discusses the difficulties encountered when attempting to run cloud transmission calculations using the point receiver estimating function in the POLO program. The spherical surface receiver estimating routine incorporated into a new version of the POLO program is described. Cloud transmission calculations using the two versions of the POLO program are compared for receivers at synchronous satellite positions and for receivers at the cloud top.

DD FORM 1 JAN 73 1473 EDITION OF 1 NOV 65 IS OBSOLETE

UNCLASSIFIED

SECURITY CLASSIFICATION OF THIS PAGE (When Data Entered)

TABLE OF CONTENTS

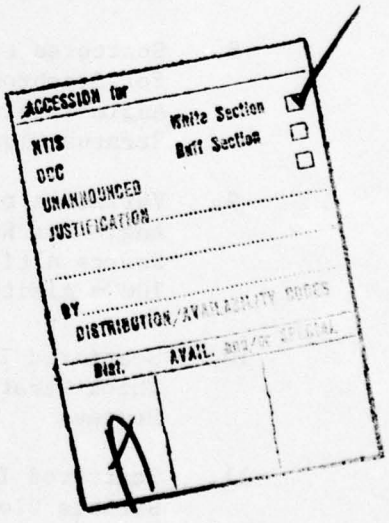

LIST OF FIGURES

LIST OF TABLES

I. INTRODUCTION

Of all atmospheric and terrain conditions affecting the transport of visible and infrared radiation through the atmosphere, cloud transmission is probably the most difficult to evaluate. This is due to the fact that a typical cloud, if such exists, is several mean-free-path lengths in thickness and the scattering phase function for cloud particles is highly anisotropic. A photon that traverses a 10- to 20-mean-free-path thick cloud will, on the average, undergo 75 to 125 collisions before escaping the cloud. Some photons will undergo as many as 200 to 300 collisions before escaping the cloud.

Figure 1 illustrates the anisotropy of light scattering within a cloud. The phase function shown in Fig. 1 is for 0.4278 μm wavelength light scattering in a stratus cloud. The phase function is highly peaked in the forward direction. The value of the phase function decreases by almost a factor of 10 from 0 to 1 degree and by more than a factor of 1000 from 0 to 10 degrees.

In the past, Radiation Research Associates, Inc. has attempted to evaluate the transmission of optical and infrared radiation through clouds using the POLO Monte Carlo program (Ref. 1). Calculations of the time-dependent scattered light intensity at satellite positions have been made for point isotropic sources located in the atmosphere below clouds of approximately 5, 14, and 20 mean-free-path lengths in thickness. For the 5 mean-free-path thick cloud, it was necessary to run approximately 25,000 photon histories to produce scattered intensities at a satellite-borne receiver that are within acceptable statistical limits. The average number of collisions required per history was approximately 40 for the 5 mean-free-path length thick cloud. The IBM 360/75 computer time required to run one problem was approximately 1 3/4 hours. Due to the excessive amounts of computer time required when using the point-receiver version of POLO, we have had to run separate problems for each receiver position.

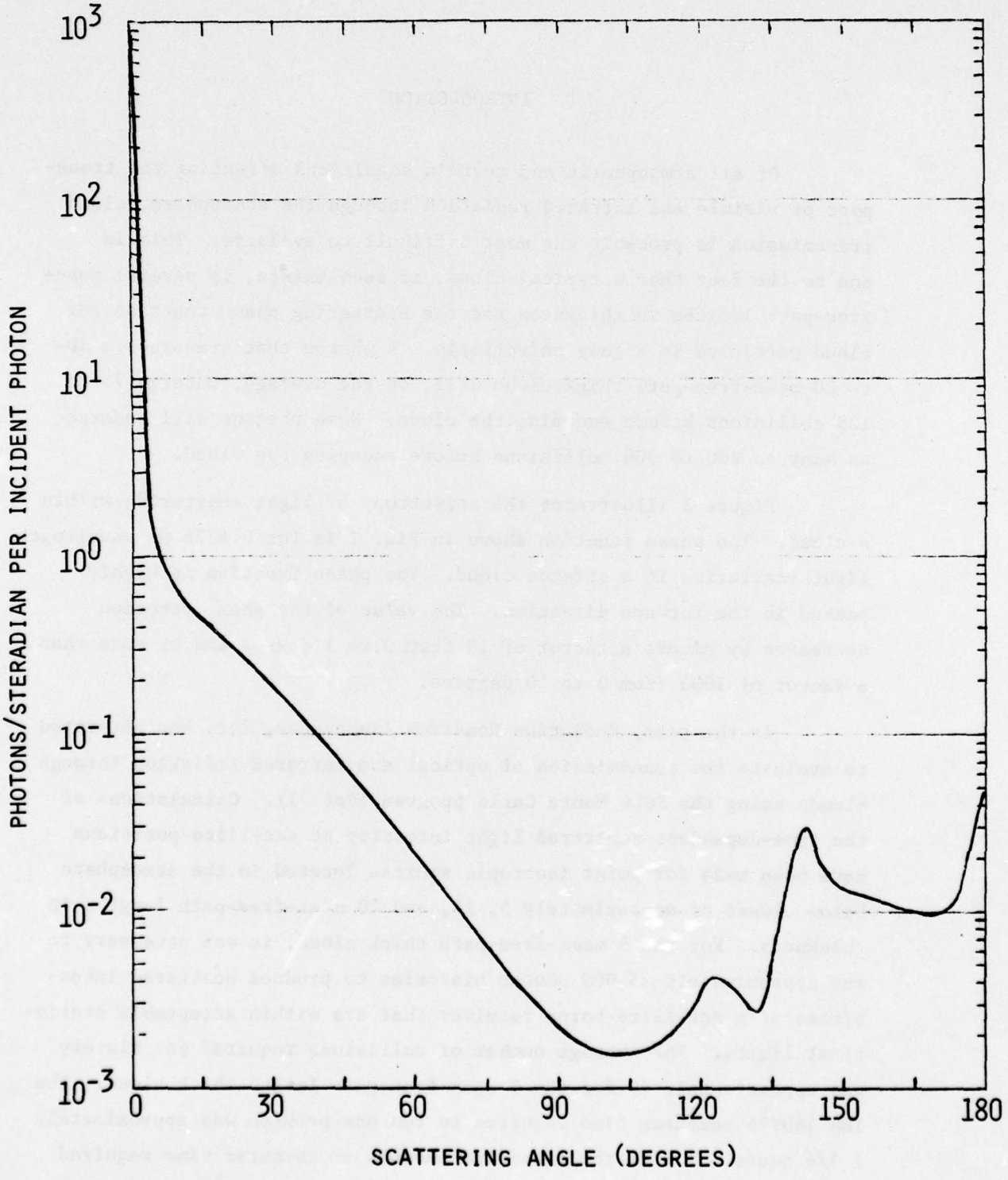

Fig. 1. Phase Function for 0.4278 μm Wavelength Light Scattering in a Stratus Cloud

After running cloud transmission problems for receivers located at satellite positions, RRA was asked by the contract monitor to determine the time, angle, and spatial distributions of the scattered light intensity at the top of a cloud located above a point isotropic source. Several attempts were made to perform these calculations using the point-receiver version of POLO. The more problems that were run, the more obvious it became that it would be impossible to run a sufficient number of histories to produce statistically reliable results.

II. POINT- AND PLANE-RECEIVER ESTIMATING FUNCTIONS

The large statistical fluctuations that occur in the results of the POLO calculations for clouds are due to the estimating function for point receivers used in the POLO program. The estimating function for a point receiver is given by the equation

$$EST = W \frac{\Sigma_S}{\Sigma_T} \frac{f(\theta)}{r^2} e^{-\Sigma_T r} \tag{1}$$

where W is the photon weight or intensity prior to scattering, $\frac{\Sigma_S}{\Sigma_T}$ is the ratio of the scattering-to-extinction coefficient, $f(\theta)$ is the phase function evaluated for the angle between the photon's direction prior to collision and the direction toward the point receiver, and r is the distance between the collision and the receiver position.

Note that if two collisions occur at the same position, but the photon directions prior to collision are different, the value of the two estimates produced by those two collisions vary directly with the values of the phase function evaluated for the two scattering angles. Since the phase function for cloud scattering is extremely peaked in the forward direction, a one-degree difference in the photon's direction prior to collision can result in a factor of 10 or more difference in the value of the phase function and thus in the estimates from the two photon collisions. Table I shows the variation of the estimates of the scattered intensity for three scattering angles and two collision-receiver separation distances. For a collision located 10 meters from the receiver, the estimate of the scattered intensity decreases from 6.17 to 4.36-3 as the scattering angle varies from 0 to 10 degrees. The value of the estimate also decreases rapidly with an increase in the distance between the collision and receiver. Increasing the collision-receiver separation distance from

TABLE I. VARIATION OF POINT RECEIVER ESTIMATOR WITH SCATTERING ANGLE AND COLLISION POSITION FOR A 15 MEAN-FREE-PATH THICK CLOUD

($\Sigma_T = \Sigma_S = .03$ 1/M, W = 1)

CLOUD THICKNESS = 500 METERS

SCATTERING ANGLE (DEG)	COLLISION-RECEIVER SEPARATION DISTANCE (METERS)	
	10	100
0°	6.17+0	4.15-3
1°	8.56-1	5.76-4
10°	4.36-3	2.93-6

10 meters to 100 meters reduces the value of the estimate by a factor of approximately 1486.

If the two effects are combined, a photon scattering through an angle of 0° toward the receiver after having a collision 10 meters from the receiver will produce an estimate 10,711 times larger than a photon scattering through a scattering angle of 1° at 100 meters from the receiver.

For receivers located several mean-free-path-length distances from the source and within the scattering medium, it is very difficult to sample collision positions near the receiver with sufficient density to provide statistically reliable results.

In order to eliminate the statistical fluctuations caused by the use of the point-receiver estimating function, the POLO program was modified replacing the point-receiver estimator with an estimating routine which gives estimates of the light intensity crossing a spherical surface. An estimate tape is written with the new POLO program giving the position, direction, time, and value of each estimate. An auxiliary program called GROPE has been written to analyze the estimate tape to determine the scattered intensity as a function of time and direction for area increments on the spherical surface.

In the modified version of POLO, the collision positions are sampled in the same manner that they were sampled in the point-receiver version of POLO. But the estimate of the intensity at the spherical surface is made after the photon's direction after scatter is selected. In the new version of POLO, the estimate is given by the expression

$$EST = W \frac{\Sigma_S}{\Sigma_T} e^{-\Sigma_T r} \Big/ \cos\gamma$$

where W is the photon weight before collision, $\frac{\Sigma_S}{\Sigma_T}$ is the ratio of the scattering-to-extinction coefficient, r is the distance from the

collision to the spherical surface along the photon direction after scattering and γ is the angle between the direction of the photon as it crosses the spherical surface and an earth radial through the point of intersection with the spherical surface.

Note that the value of the estimate does not vary with the scattering angle. Neither is the value of estimate as highly dependent upon the distance from the collision to the receiver surface as it was for the point receiver because the $1/r^2$ term is removed. Therefore, the statistical variation in the estimates of the intensity at a spherical surface receiver should be less than that which occurs when making estimates for a point receiver.

Of course, the average of the estimates crossing a spherical surface area is not equivalent to the scattered intensity at a point receiver since the area of the surface is usually fairly large compared to the detection area of a point receiver. In order to determine the scattered intensity at a particular point on the receiver surface, an area on the spherical surface surrounding the point may be designated to represent the point and the average of the estimates crossing the spherical surface within that area can be used to predict the radiation intensity at the point of interest. If the scattered intensity does not vary radically with position, the statistical fluctuation of the estimates can be reduced by increasing the size of the area used to represent the point.

Each estimate computed with the modified POLO program is recorded on an estimate file along with the location of the estimate position on the spherical surface, the time of crossing the surface, and the direction of the photon as it crosses the surface. The position and direction angles used to record the position crossed on the spherical surface and the direction of motion of the photon are shown in Fig. 2. The estimate file is saved for future analysis with the GROPE program which sorts and averages the estimates within designated area, time, and angle intervals.

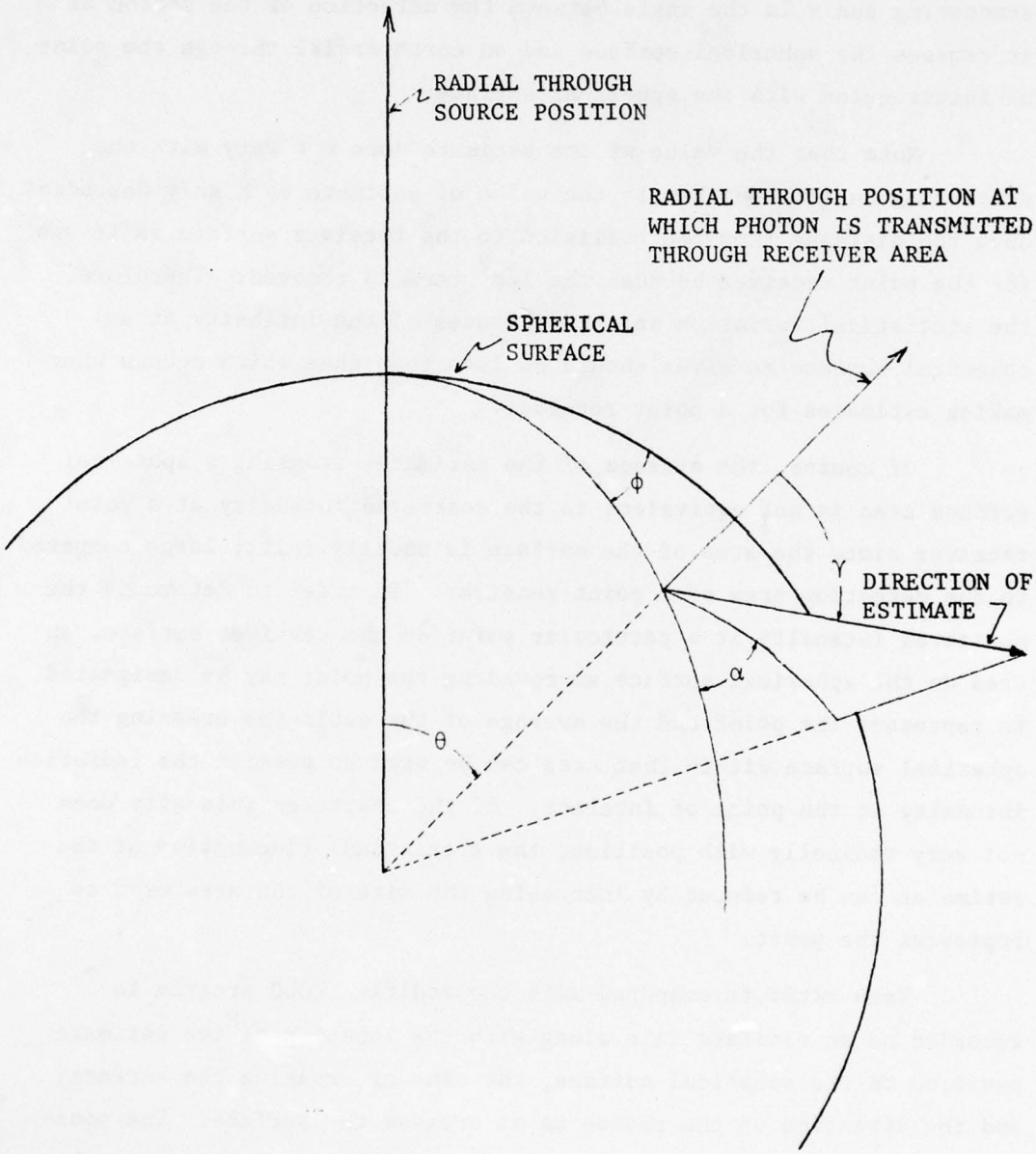

Fig. 2. Position and Direction Angle of an Estimate

A preliminary analysis of the estimates of the scattered radiation at the spherical surface is also performed within the modified *POLO program*. The time dependence of the scattered light intensity integrated over all directions is obtained for annular area increments on the spherical surface. *Figure 3 shows how the incremental* areas on the spherical surface are defined.

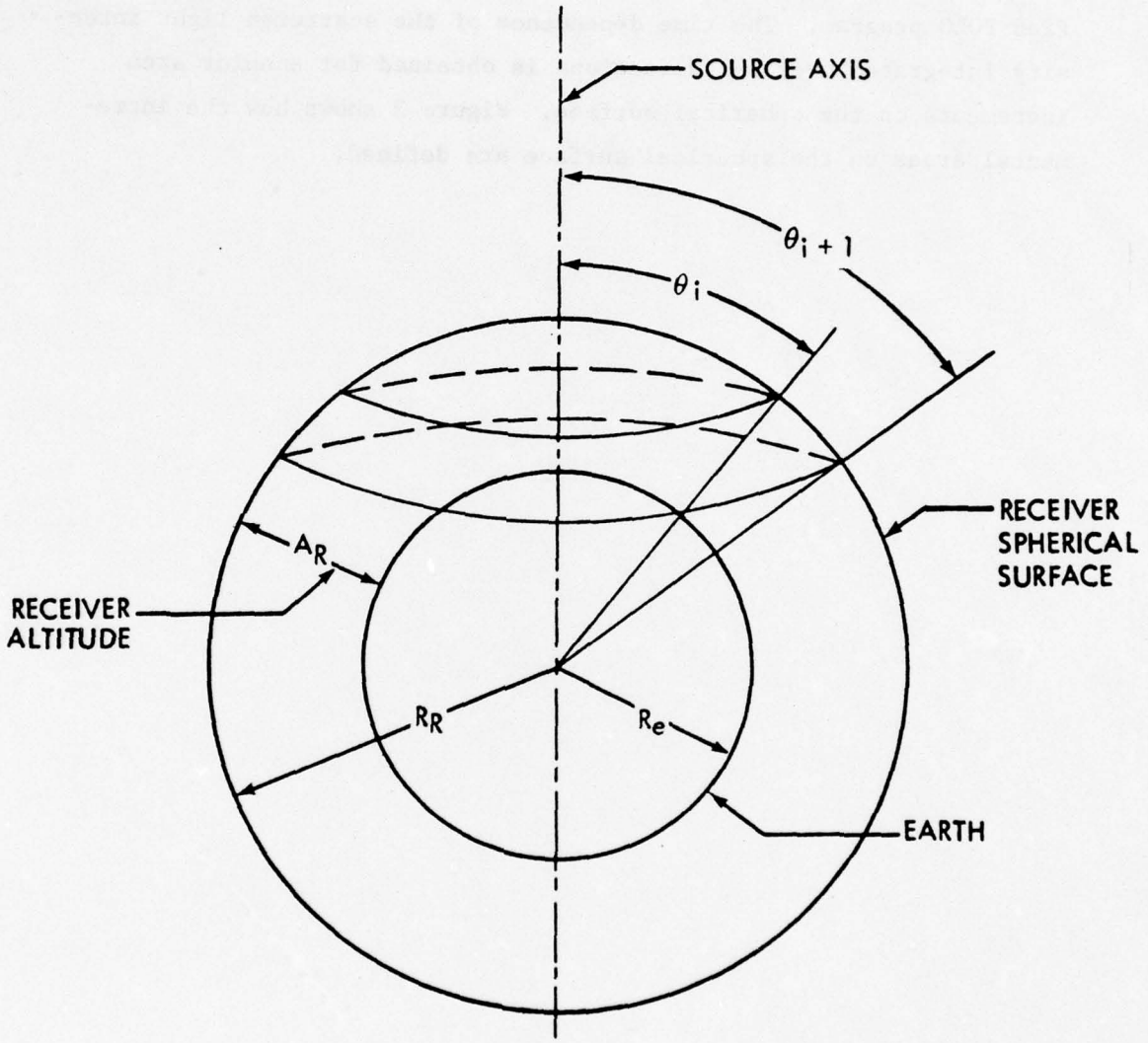

Fig. 3. Spherical Surface Receiver Areal Definition

III. CLOUD TRANSMISSION CALCULATIONS

Three test problems have been run with the modified version of POLO to compare with results from the point-receiver version and to compare the efficiency of the two versions.

In two of the problems, a 0.4278 μm wavelength point isotropic source was located at the lower surface of a 5 mean-free-path thick stratus cloud extending from 500 to 1,000 meters altitude. In one test problem, receivers were located at a synchronous satellite altitude of 35,800 kilometers while in the other test case the receivers were located at the cloud top which was at 1,000 meters altitude. Figure 4 shows the scattered radiation intensity at a synchronous altitude plotted versus look angle as obtained from calculations made with both the point receiver and the spherical-area receiver versions of POLO. Note that the results obtained from the point-receiver calculations are higher than those obtained from the spherical surface receiver calculations. In the spherical receiver problem, it was assumed there was no atmosphere above the cloud, but in the point-receiver problem there was approximately one-half of a mean-free-path length of atmosphere above the cloud top. It is believed that this difference in the atmospheric models is the reason for the difference in magnitude of the scattered intensity as given by the two different calculations. Twenty-five thousand photon histories were run to obtain the results for each of the three point receivers, while only 10,000 histories were run to obtain the histogram shown in Fig. 4 for the spherical surface receiver results. Approximately 13 minutes CPU time was used in generating the histogram for the spherical surface receiver, while over 5 1/2 hours CPU time was used in the point-receiver calculation. The time distribution of the scattered intensity at the 0-degree look angle is compared in Fig. 5 for the two different types of receivers. The lines represent the data computed with the point-receiver calculation, while the point data are

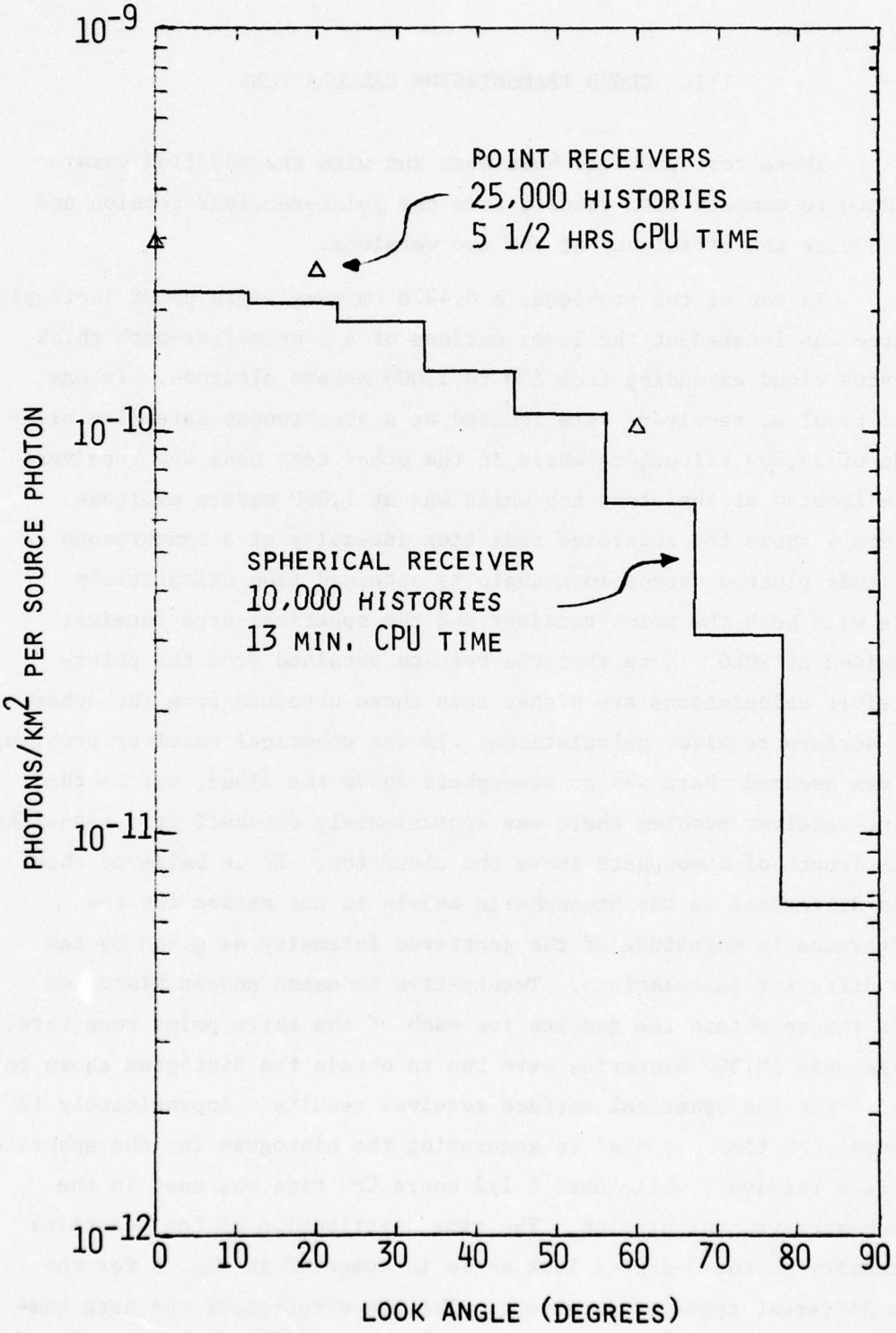

Fig. 4. Scattered Intensity Versus Look Angle at Synchronous Satellite Altitude

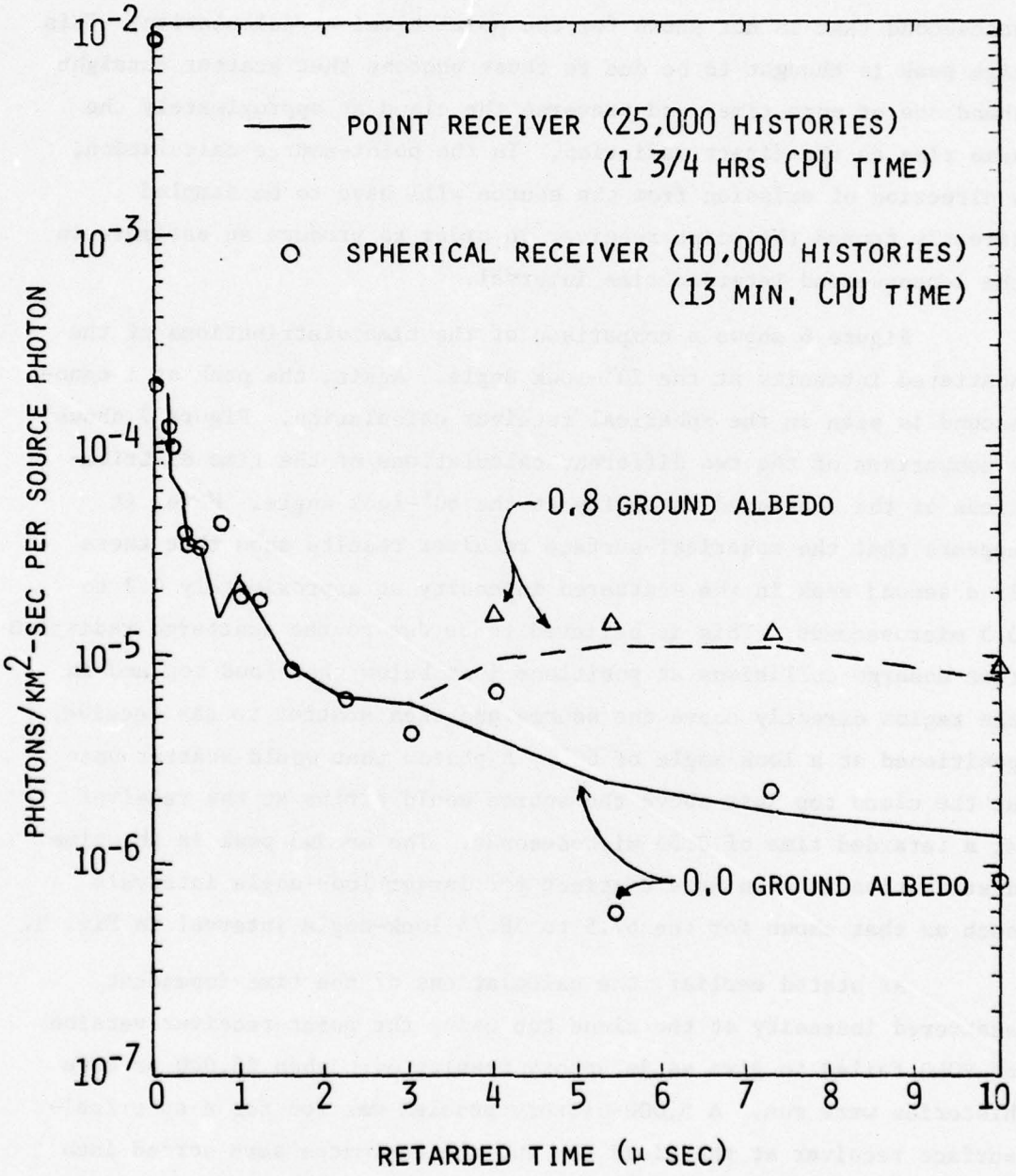

Fig. 5. Scattered Intensity Versus Retarded Time for Synchronous Satellite at 0° Look Angle Above 5 Mean-Free-Path Thick Stratus Cloud

that obtained from the spherical-receiver calculations. Note that the spherical surface receiver calculation shows a high peak at 1 nanosecond that is not shown for the point-receiver calculation. This high peak is thought to be due to those photons that scatter straight ahead one or more times and traverse the cloud at approximately the same time as the direct radiation. In the point-source calculation, a direction of emission from the source will have to be sampled directly toward the point receiver in order to produce an estimate in the 1-nanosecond retarded time interval.

Figure 6 shows a comparison of the time distributions of the scattered intensity at the 20°-look angle. Again, the peak at 1 nanosecond is seen in the spherical receiver calculation. Figure 7 shows a comparison of the two different calculations of the time distributions of the scattered intensity at the 60°-look angle. Here, it appears that the spherical-surface receiver results show that there is a second peak in the scattered intensity at approximately 0.2 to 0.3 microseconds. This is believed to be due to the scattered radiation that undergo collisions at positions just below the cloud top and in the region directly above the source and then scatter to the receiver positioned at a look angle of 60°. A photon that would scatter once at the cloud top just above the source would arrive at the receiver at a retarded time of 0.55 microseconds. The second peak in the time distribution is even more distinct for larger look-angle intervals such as that shown for the 67.5 to 78.75 look-angle interval in Fig. 8.

As stated earlier, the calculations of the time-dependent scattered intensity at the cloud top using the point-receiver version of POLO failed to give satisfactory results even when 25,000 or more histories were run. A 5,000-history problem was run for a spherical-surface receiver at the cloud top and the estimates were sorted into look-angle intervals out to 90 degrees. The results for the spherical-surface receivers are compared with the point receiver data in Fig. 9. The 5,000 histories run to compute the data plotted as a histogram

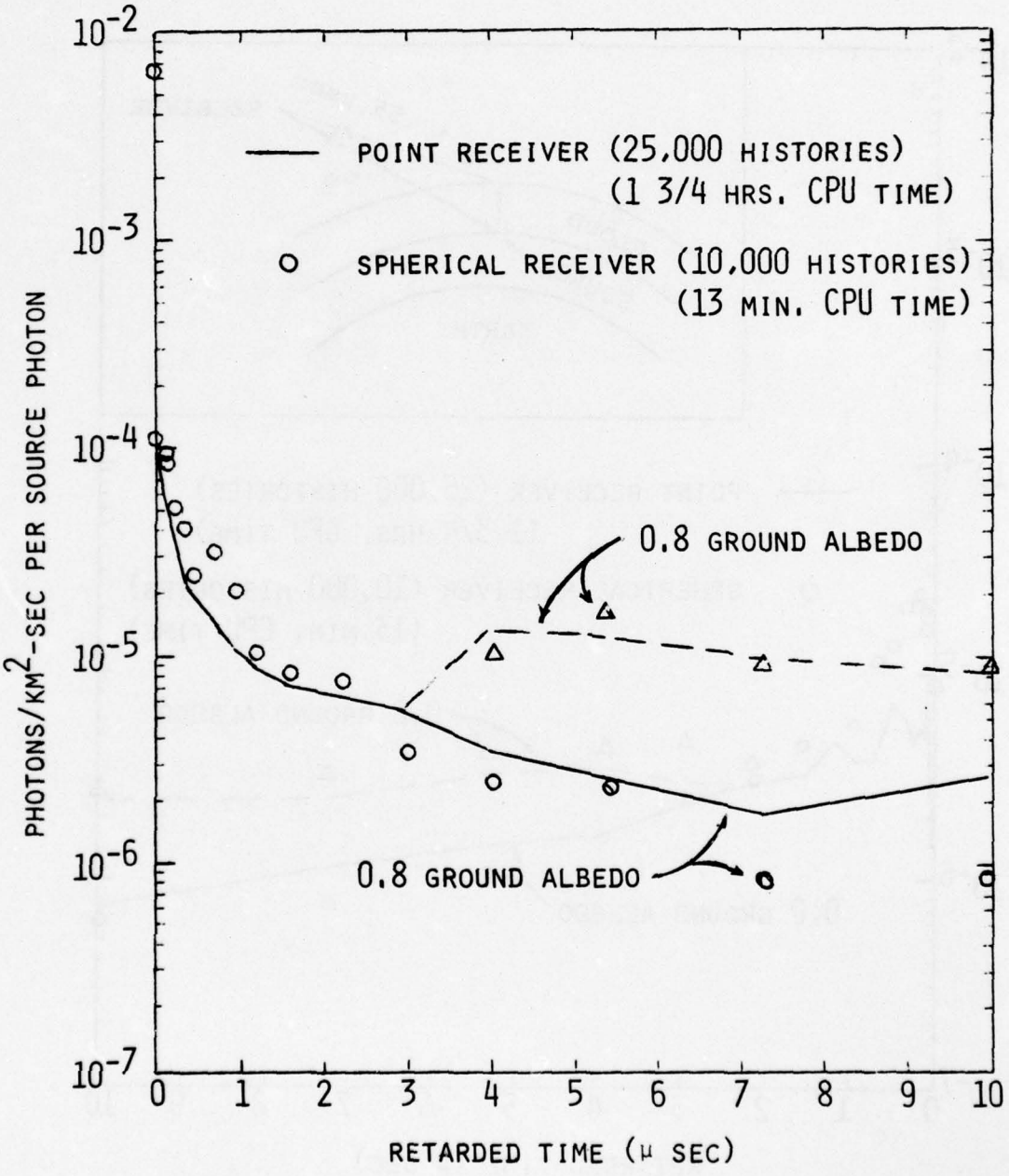

Fig. 6. Scattered Intensity Versus Retarded Time for Synchronous Satellite at 20° Look Angle Above 5 Mean-Free-Path Thick Stratus Cloud

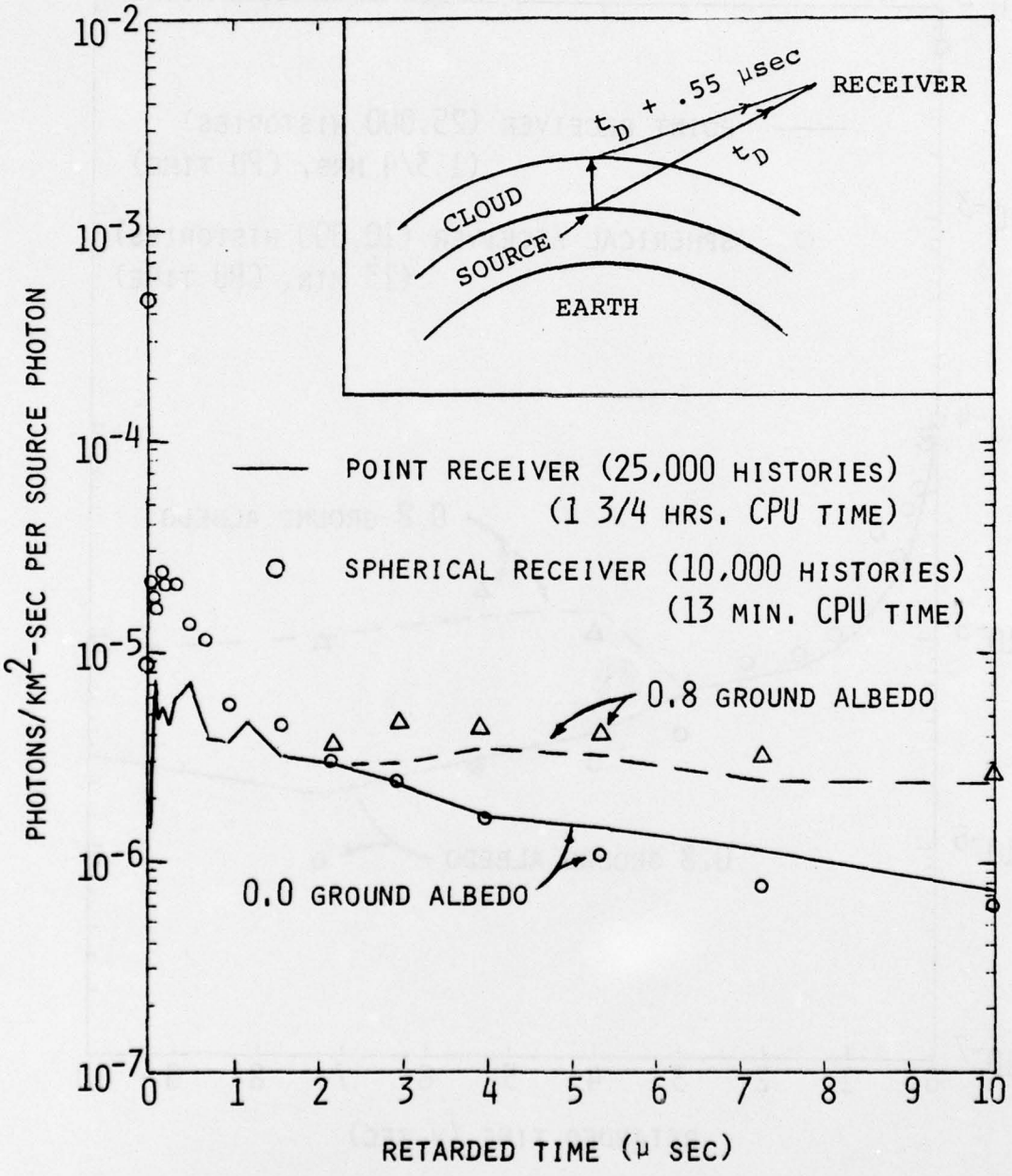

Fig. 7. Scattered Light Intensity Versus Retarded Time for Synchronous Satellite at 60° Look Angle Above 5 Mean-Free-Path Thick Stratus Cloud

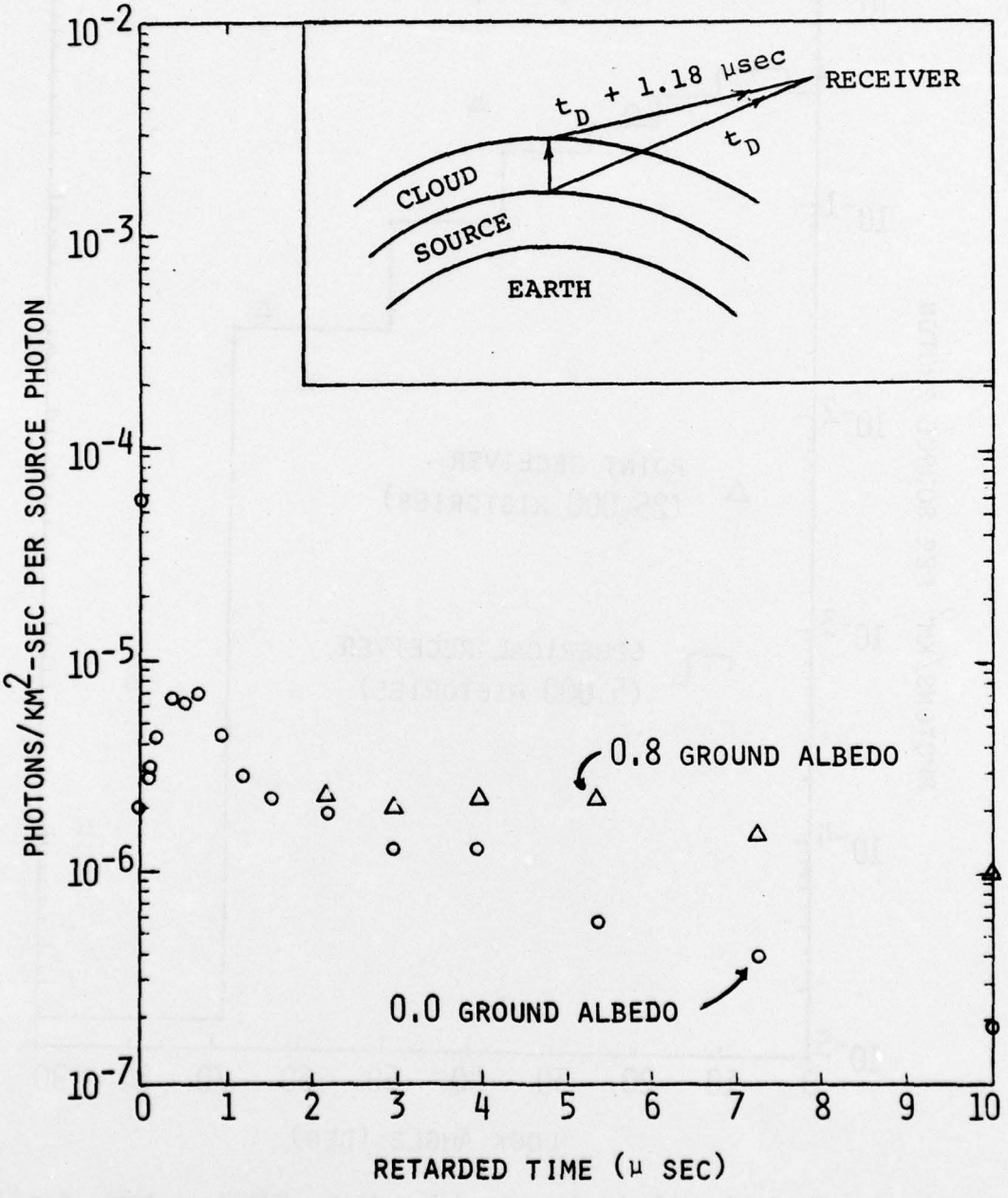

Fig. 8. Scattered Light Intensity Versus Retarded Time for Synchronous Satellite at 67.5 - 78.75 Look Angle Interval Above 5 Mean-Free-Path Thick Stratus Cloud

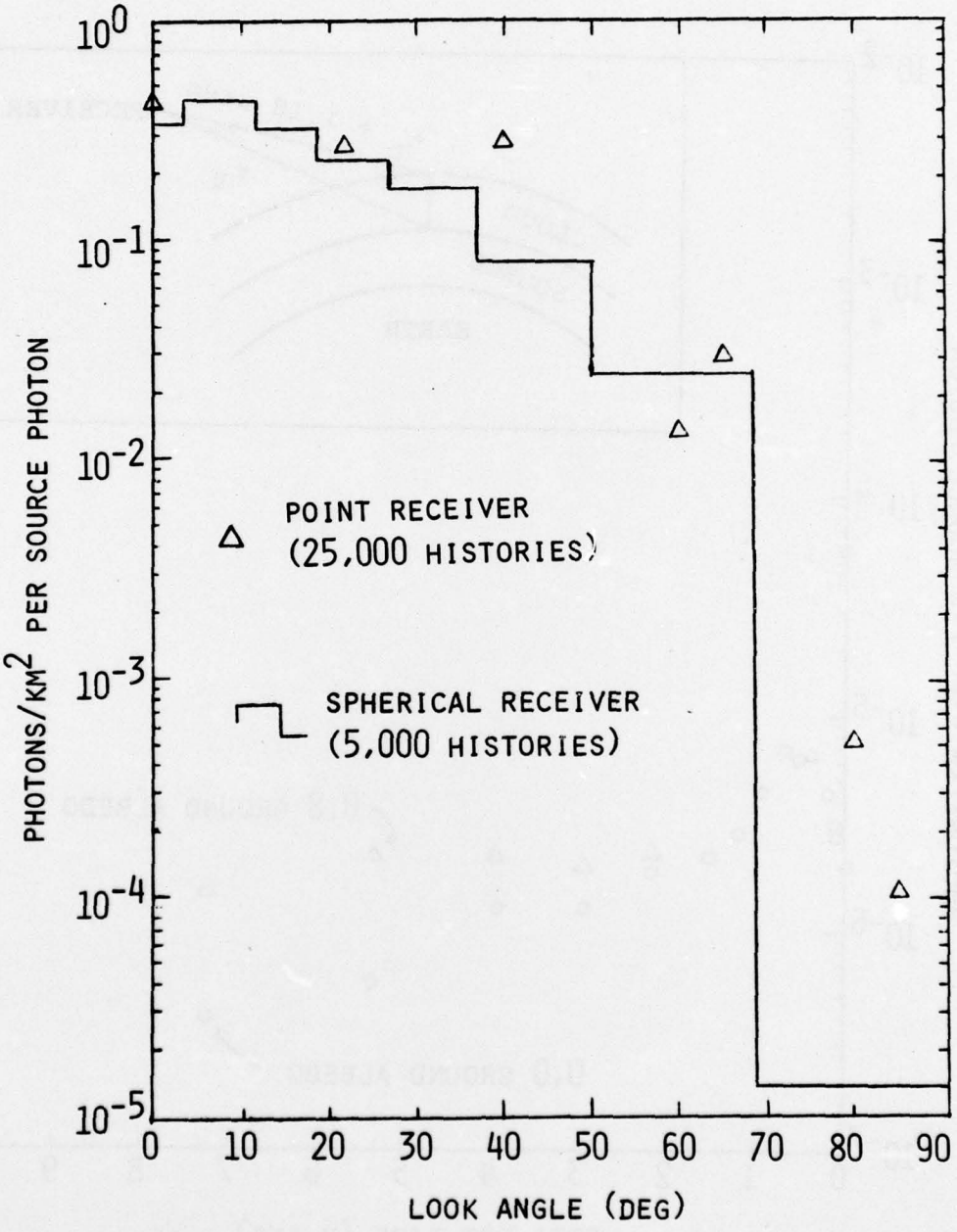

Fig. 9. Variation of the Scattered Intensity with Look Angle for Receivers at Cloud Top: λ = .4278μ, Source Altitude = 500m, Cloud at 500m to 1000m Altitude

required about 6 1/2 minutes CPU time, whereas, the point data shown required about six hours of CPU time. The point-receiver data shown in Fig. 9 are averages of the data from several POLO runs which utilized different biasing techniques in an effort to reduce computer time and improve the statistical accuracy of the calculated intensities. Even though about six hours of CPU time were expended in this effort, each of the results from the individual runs, as well as the combined results, still show large statistical fluctuations. The fluctuations in the time- and angle-dependent scattered intensities were so large that it was difficult to observe any trends in those distributions. The spherical-receiver data appears to have less statistical fluctuation than the point-source calculations, even though the spherical-receiver data were generated with only a fraction of the machine time. There is no logical explanation for the scattered intensity to be higher at 65 degrees than at 60 degrees, so this is attributed to statistical fluctuation in the point-receiver data. The time distributions of the spherical-receiver data have less statistical fluctuation for the larger look anlges because the areas used to represent the receiver positions were allowed to increase with an increase in the look angle. The time distribution of the scattered intensity at the cloud top in the 36.8- to 50.36-degree look angle interval is compared with that obtained for a point receiver at 40° in Fig. 10. The time distribution of the scattered intensity calculated with the point-receiver version of POLO appears to be higher than that calculated with the spherical-receiver version. The time-integrated intensity that was computed with the point-receiver version of POLO also appears to be high in Fig. 9. The erratic nature of the time-dependent scattered intensity calculated with the point-receiver version of POLO illustrates the difficulty encountered in attempting to compute statistically reliable data with the point-receiver version of POLO when the receivers are located within the atmosphere. Figure 11 shows another comparison between the calculations using the point and spherical receiver versions of POLO. Again, the statistical fluctuation of the point-receiver calculation appears to be much larger than that of

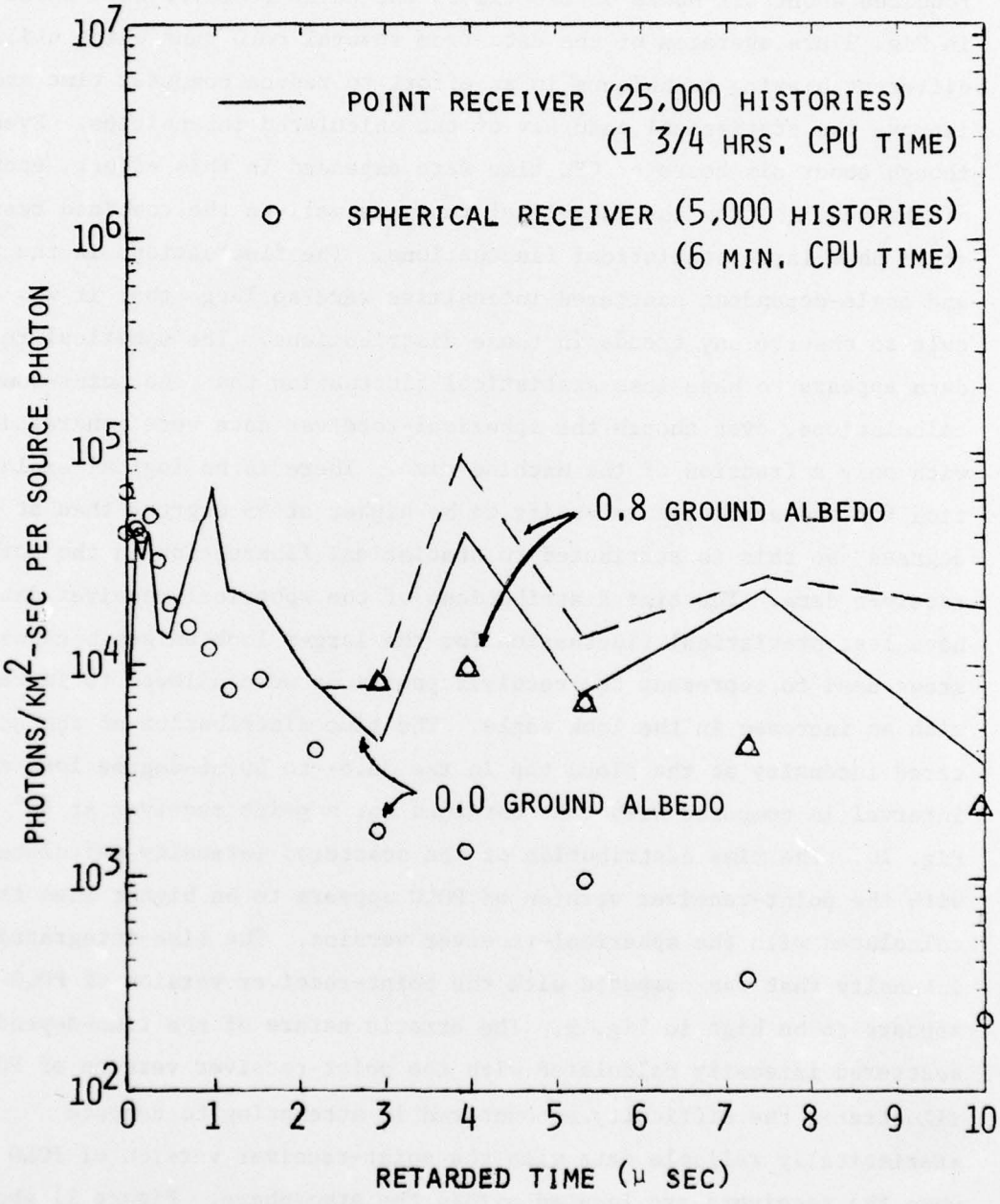

Fig. 10. Scattered Intensity at Top of 5 Mean-Free-Path Thick Stratus Cloud for a Look Angle of 40 Degrees

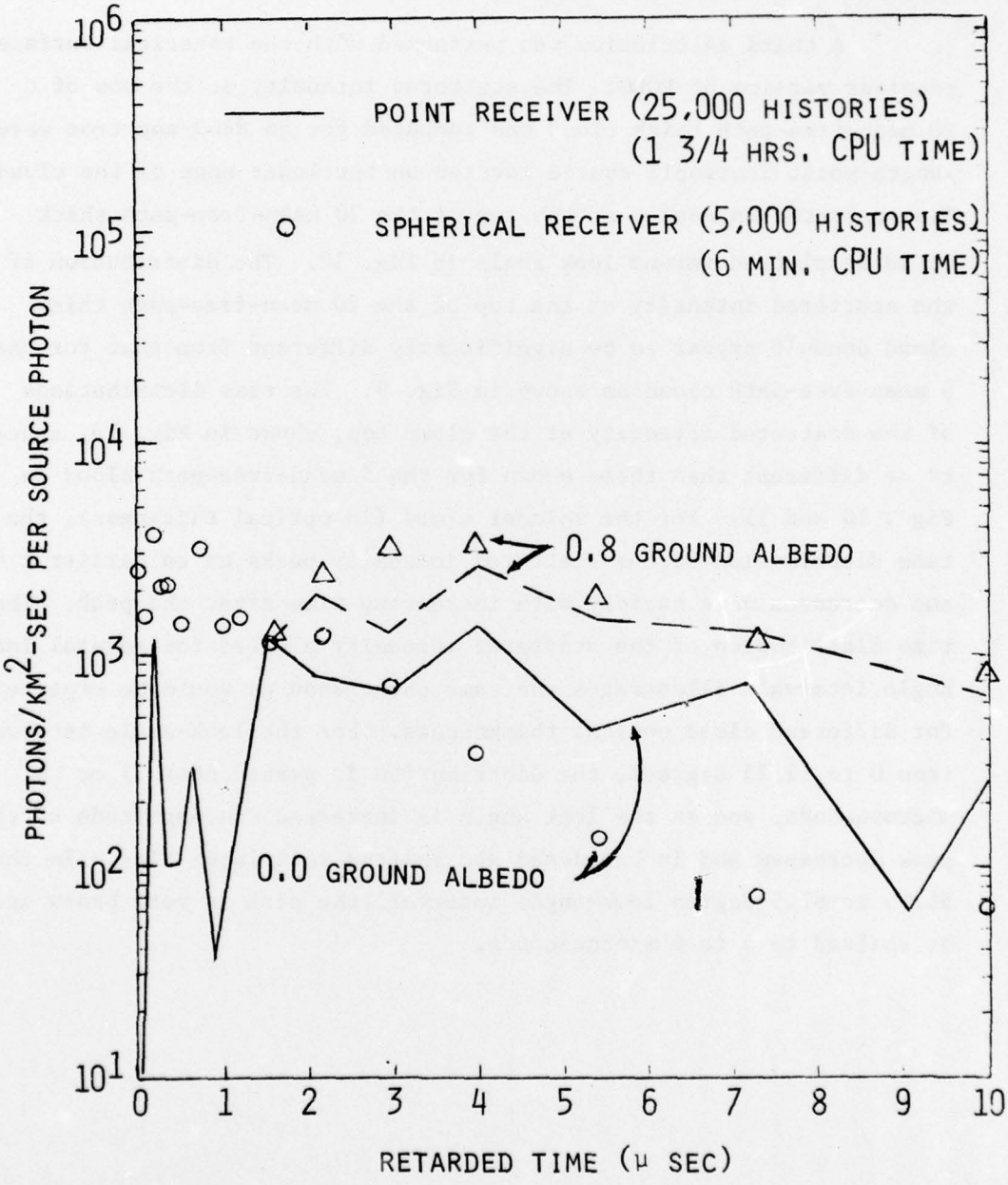

Fig. 11. Scattered Intensity at Top of 5 Mean-Free-Path Stratus Cloud for a Look Angle of 60 Degrees

the spherical surface receiver calculation even though much more computer time was spent in generating the point-receiver results.

A third calculation was performed with the spherical surface receiver version of POLO. The scattered intensity at the top of a 20 mean-free-path thick cloud was computed for an 8400-angstrom wavelength point isotropic source located on the lower edge of the cloud. The scattered intensity at the top of the 20 mean-free-path thick cloud is plotted versus look angle in Fig. 12. The distribution of the scattered intensity at the top of the 20 mean-free-path thick cloud doesn't appear to be significantly different from that for the 5 mean-free-path cloud as shown in Fig. 9. The time distributions of the scattered intensity at the cloud top, shown in Fig. 13, appear to be different than those shown for the 5 mean-free-path cloud in Figs. 10 and 11. For the thinner cloud (in optical thickness), the time distribution of the scattered intensity peaks at an earlier time and decreases more rapidly with increasing time after the peak. The time distribution of the scattered intensity plotted for several look-angle intervals illustrates the same phenomenon as would be expected for different cloud optical thicknesses. For the look-angle interval from 0 to 11.25 degrees, the distribution is peaked near .3 or .4 microseconds, and as the look angle is increased the magnitude of the peak decreases and is broadened and shifted to a later time. In the 56.25 to 67.5 degree look-angle interval, the peak is very broad and is shifted to 5 to 6 microseconds.

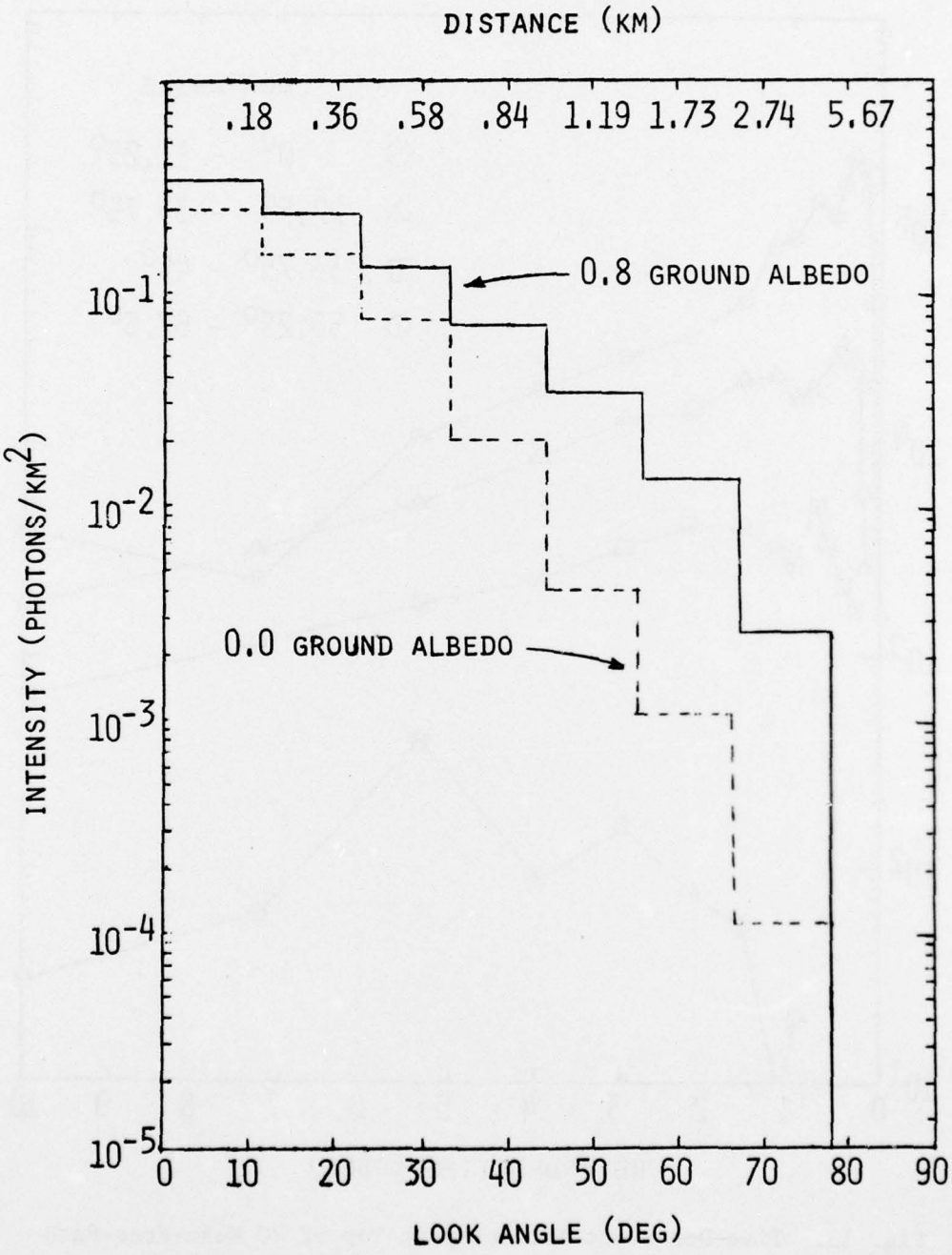

Fig. 12. Intensity Distribution at Top of 20 Mean-Free-Path Thick Cloud for 8400 Angstrom Wavelength Light

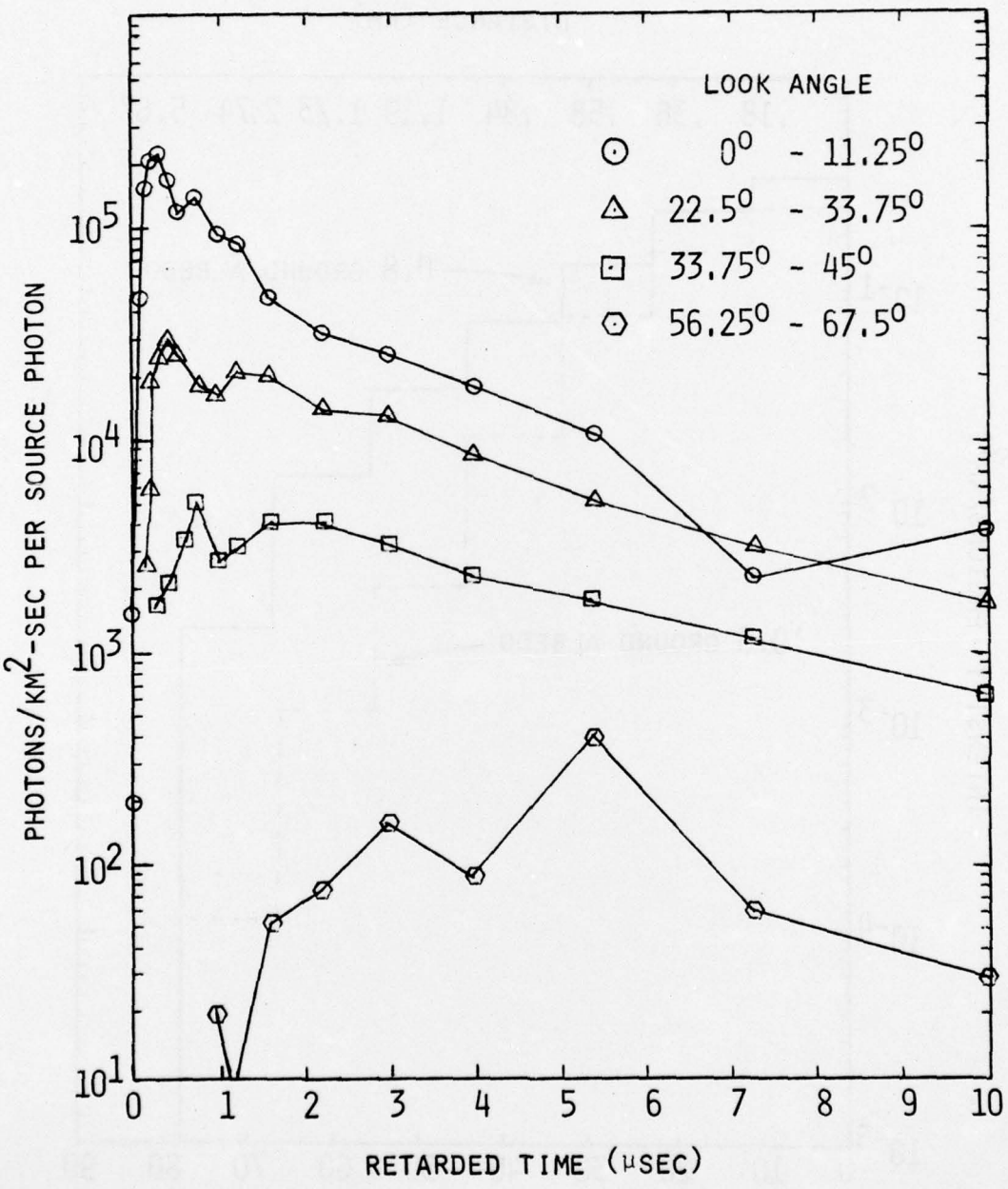

Fig. 13. Time-Dependent Intensity at Top of 20 Mean-Free-Path Thick Cloud for 8400 Angstrom Wavelength Light (Ground Albedo = 0.0)

IV. CONCLUSIONS

Using the spherical surface receiver estimator will reduce the statistical fluctuation in the POLO Monte Carlo calculations of cloud transmission and provide more accurate transmission data with a smaller amount of computer time. The spherical surface receiver version of the POLO program provides a more accurate definition of the time distribution of the scattered light intensity at very early times, i.e., in the nanosecond and 10's of nanoseconds of retarded time. This is because the photons that scatter straight ahead one or more times and reach the receiver at approximately the same time as the direct intensity are seen with the spherical surface receiver calculations. Those photons will not be seen with the point-receiver version of POLO unless directions of emission from the source are sampled along the line-of-sight between the source and receiver.

The time distribution of the scattered intensity for receivers at large look angles at synchronous satellite positions appeared to have two peaks. A sharp peak occurred at 1 nanosecond due to those photons scattering straight ahead along the line-of-sight between the source and receiver and a second broader peak at a few tenths of a microsecond which is thought to be due to those photons that undergo collisions in a region near the cloud top that is directly above the source position.

REFERENCES

1. D. G. Collins and M. B. Wells, A Study of Thermal Radiation Propagation in the Atmosphere, Radiation Research Associates, Inc. Technical Report RRA-T7011 (August 1970)

DISTRIBUTION

No of Copies	
	DOD AGENCIES
2	Director Defense Nuclear Agency ATTN: RAAE Technical Library
2	Director Defense Intelligence Agency ATTN: Nuclear Energy Division Technical Library
12	Defense Documentation Center ATTN: Document Control
2	Director Defense Advanced REsearch Projects Agency ATTN: NMRO TIO
	ENERGY RESEARCH AND DEVELOPMENT ADMINISTRATION
5	Los Alamos Scientific Laboratory ATTN: J-10 (Dr H. Horak) J-10 (Dr Guy Barasch) T-12 (Dr D.C. Cartwright) TD-3 (Dr Bob Henson) Technical Library
1	ERDA/DMA ATTN: Mr D. Gale
3	Sandia Laboratories ATTN: Dean Thornbrough Bob Bradley Reports Collection
1	Lawrence Livermore Laboratory ATTN: Technical Library
1	Oak Ridge National Laboratory ATTN: Technical Library
1	EG&G, Inc. Bedford MA ATTN: Technical Library
1	EG&G, Inc. Los Alamos NM ATTN: Dr C. Mitchell
	DEPARTMENT OF THE ARMY
1	Army Nuclear Effects Lab ATTN: Technical Library
2	US Army Electronics Command ATTN: Technical Library Dr. R. Buser
1	US Army Combat Developments Command-Institute of Nuclear Studies ATTN: Technical Library
2	US Army Waterways Experiment Station-Mobility and Environmental System Lab ATTN: Dr. L.E. Link Dr. Warren Grabau
3	US Army Electronics Command Atmospheric Sciences Laboratory ATTN: Dr M.L. Vatsia Dr Jerry Lentz Dr Richard Gomez
1	US Army Missile and Development Command-Physical Sciences Directorate ATTN: Dr Julius Lilly
2	Ballistic Research Laboratory ATTN: Mr. Norman Banks Mr. Ennis Quigley

No of Copies

DEPARTMENT OF THE NAVY

1 Naval Research Laboratory
ATTN: Technical Library

1 Naval Postgraduate School
ATTN: Technical Reports Librarian

2 Naval Surface Weapons Center
ATTN: Mr Williard Derksen
Mr Barry Katz

1 Naval Ordnance Test Station
ATTN: Dr. Richard Bird

DEPARTMENT OF THE AIR FORCE

4 AF Geophysics Laboratories
ATTN: OPR (Mr H. Gardiner)
OPA (Dr R. Fenn)
OPR (Dr A. T. Stair)
Research Library

1 AF Institute of Technology
ATTN: Library

4 AF Weapons Laboratory
ATTN: Dr Joe Janni
Mr Al Sharp
Dr C. Needham
Technical Library

1 Space and Missile Systems Organization
ATTN: SZS (Maj H. Hayden)

2 AF Technical Applications Center
ATTN: TFR (Capt J. Lange)

1 AFETAC
ATTN: DNE (Capt L. Mendenhall)

No of Copies

DOD CONTRACTORS

3 Aerospace Corporation
ATTN: Dr R.D. Rawcliffe
Dr Kelly Spearman
Library Services

1 Analytical Systems Corporation
ATTN: Dr I. Kohlberg

1 Battelle Memorial Institute
ATTN: Radiation Effects Information Center

1 AVCO - Everett Research Laboratory
ATTN: Technical Library

1 General Electric Company-TEMPO
ATTN: DNA Information and Analysis Center

1 Kaman Sciences Corporation
Kaman Nuclear Division
ATTN: Technical Library

1 Lockheed Missiles and Space Company
ATTN: Technical Library

1 The MITRE Corporation
ATTN: Technical Library

1 The RAND Corporation
ATTN: Technical Library

1 R&D Associates
ATTN: Technical Library

1 Stanford Research Institute
ATTN: Technical Library

No of Copies	
1	TRW Systems Group ATTN: Technical Information Center
1	Visidyne, Inc. ATTN: Dr. J. Carpenter
1	Mission Research Corporation ATTN: Technical Library
1	*Teledyne Brown Engineering*
1	Science Applications, Inc. ATTN: Dr R. Hillendahl
1	HSS, Inc. ATTN: Dr H. Stewart
20	Radiation Research Associates ATTN: M.B. Wells
1	Bendix Engineering Corporation Grand Junction Operations ATTN: Dr Peter Alexander
1	Institute for Defense Analyses ATTN: Technical Information Office